NASA Technical Memorandum 107518
AIAA–97–3144

Army Research Laboratory
Technical Report ARL–TR–1462

Passage-Averaged Description of Wave Rotor Flow

Gerard E. Welch and Louis M. Larosiliere
U.S. Army Research Laboratory
Lewis Research Center
Cleveland, Ohio

Prepared for the
33rd Joint Propulsion Conference and Exhibit
cosponsored by AIAA, ASME, SAE, and ASEE
Seattle, Washington, July 6–9, 1997

National Aeronautics and
Space Administration

U.S. ARMY
RESEARCH LABORATORY

Passage-Averaged Description of Wave Rotor Flow

Gerard E. Welch* and Louis M. Larosiliere*
Army Research Laboratory
NASA Lewis Research Center
21000 Brookpark Road, M/S 77-7
Cleveland, OH 44135

The unsteady flow within wave rotor passages is influenced by the rotor blade, hub, and tip-shroud surface profiles. By averaging from hub to shroud and from blade to blade, a reduced set of the governing equations is obtained that is appropriate for design studies and parametric analyses. The application of these equations requires closure models for force integrals and for correlation terms that arise when the density-averages of products of the flow field variables are expanded in terms of products of the density-averaged variables. The force integrals and the correlation terms depend on the instantaneous pitchwise and spanwise flow field distributions established by unsteadiness relative to the rotor, flow turning induced by blade, hub, and tip-shroud profiling, and rotation. Two approaches to model the force integrals are described. The influence of relative unsteadiness and flow turning on the correlation terms is discussed by considering the propagation of gas dynamic waves in rotor passages defined by uncambered, staggered blades and by unstaggered, cambered blades.

Nomenclature

a = $(\gamma p/\rho)^{1/2}$, speed of sound
$\hat{e}$ = unit vector
$\tilde{e}_I$ = $\tilde{h}_I - (p/\rho)$, specific relative energy
$\underline{F}$ = inviscid flux vector
$\underline{F}'$ = flux vector of correlation terms
$\underline{G}$ = source vector
G_4' = correlation terms of radial source terms
$\tilde{h}_I$ = $\tilde{h} - r\Omega u_\theta$, specific rothalpy
$\tilde{h}$ = $\frac{\gamma}{\gamma-1}p/\rho + \frac{1}{2}(\underline{u}\cdot\underline{u})$, specific total enthalpy
$\underline{L}$ = vector of force integrals
L_R = axial length of rotor
L_T = rotor chord length
L_W = rotor pitch
p = static pressure
$\underline{Q}$ = vector of conserved variables
$\underline{R}$ = (R,μ), polar coordinate system of Fig. 3
$\underline{r}$ = (r,θ,z), position vector relative to spinning rotor
S = passage cross-sectional area (cf. Eq. 5).
t = time
$\underline{u}$ = absolute velocity (*e.g.*, (u_r,u_θ,u_z))
$\underline{w}$ = $\underline{u} - \Omega r\hat{e}_\theta$, relative velocity (*e.g.*, (w_r,w_θ,w_z))
w_{SH} = relative speed of shock wave (see fig 1).
z^* = normalized axial distance (see Figs. 1-3)
β = $\tan^{-1}(w_\theta/w_z)$, relative swirl angle
γ = ratio of specific heats
Δ_θ = $\Delta_\theta(\varphi) = \varphi_P - \varphi_S$, pitchwise difference
Δ_r = $\Delta_r(\varphi) = \varphi_T - \varphi_H$, spanwise difference
ϵ^r = ratio of static pressures across expansion fan
σ = L_T/L_W, solidity
$\underline{\xi}$ = (ξ,η), intrinsic coordinates
ρ = mass density
ϕ = $\tan^{-1}(w_r/w_z)$, meridional flow angle
Ω = shaft angular speed
$\overline{}$ = denotes an area-average (cf. Eq. 5)
$\langle\rangle$ = denotes a density-weighted average (cf. Eq. 6)

Subscripts

H = rotor hub
P = rotor passage leading blade-surface
S = rotor passage trailing blade-surface
T = rotor tip-shroud
0 = rotor passage initial relative conditions
1 = rotor passage inlet (or exit) relative conditions

Introduction

The wave rotor is a member of the family of dynamic pressure exchange devices.[1] It consists of a shrouded rotor surrounded by a stationary casing. The casing endwalls are penetrated in sectors by inlet and outlet ducts that port gas to and from the rotor flow annuli. Gas dynamic waves are initiated and terminated as the rotor passages open and close to the ported flows.

---

*Vehicle Technology Center; member AIAA.

Wave rotors are self-cooling and can therefore be used to top turbine-inlet-temperature-limited gas turbine engines.[2] Recent research has emphasized axially bladed wave rotors (*i.e.*, pressure-exchangers); however, engine performance levels might be enhanced more significantly by topping with wave rotors that produce net shaft power (*i.e.*, wave engines or wave turbines).[3,4]

Motivated by this potential advantage, a design/analysis tool is currently needed which is able to predict accurately the performance of wave rotors with arbitrary passage geometries. One-dimensional wave rotor flow solvers suitable for parametric analyses can be used to predict the performance of pressure-exchangers accurately;[5] however, there are no comparable computational tools available for the generalized rotor passage geometries of wave engines. Although multi-dimensional flow solvers[6,7] can be used to compute the wave rotor flow field in complicated geometries, it is currently impractical to perform the parametric analyses of design studies with these tools.

The purpose of the present work is to formulate a passage-averaged description of wave rotor flow which accounts for blade stagger and camber, and hub and tip-shroud profiling in a reduced-dimension model suitable for parametric analysis tools. The paper proceeds as follows: 1.) the passage-averaged formulation is obtained by pitchwise- and spanwise-averaging of the Euler equations; 2.) closure models for the blade force integrals resulting from the averaging procedure are provided; and 3.) the influences of relative unsteadiness and relative flow turning on correlation terms introduced in application of the passage-averaged equations are discussed by using analysis of the flow fields established by the propagation of gas dynamic waves in idealized wave rotor passages.

Passage-Averaged Model

Wave rotors are currently envisaged to be axial or mixed-flow machines. Influenced by the rotor geometry, the Euler equations are averaged from hub to tip and from blade to blade in this work. This averaging procedure yields a set of equations with one (axial) space derivative suitable for a CFD-based wave rotor analysis tool.

Governing Equations

The mass, momentum (component in an arbitrary direction $\hat{e}_i$), and energy equations for an inviscid flow written in a frame of reference that is rotating with the rotor are

$$\frac{\partial \rho}{\partial t} + \nabla\cdot(\rho \underline{w}) = 0 \qquad (1)$$

$$\frac{\partial \rho (\underline{w}\cdot\hat{e}_i)}{\partial t} + \nabla\cdot(\rho \underline{w}(\underline{w}\cdot\hat{e}_i)) + \hat{e}_i\cdot\nabla p = \rho[(\Omega^2 \underline{r} - 2\underline{\Omega}\times\underline{w})\cdot\hat{e}_i + \underline{w}\cdot\frac{D\hat{e}_i}{Dt}] \qquad (2)$$

and

$$\frac{\partial \rho \tilde{e}_I}{\partial t} + \nabla\cdot(\rho \underline{w}\tilde{h}_I) = 0 \quad , \qquad (3)$$

respectively. In cylindrical coordinates, for example, $D\hat{e}_r/Dt = w_\theta \hat{e}_\theta / r$, $D\hat{e}_\theta/Dt = -w_\theta \hat{e}_r/r$, and $D\hat{e}_z/Dt = 0$.

Averaged Equations

By averaging Eq. 1 from hub to tip and from blade to blade in cylindrical coordinates it is found that

$$\frac{\partial \bar{\rho} S}{\partial t} + \frac{\partial \bar{\rho} S <w_z>}{\partial z} = 0 \qquad (4)$$

where the area- and density-averages are defined by

$$\overline{\psi} \equiv \frac{\int_{r_H}^{r_T}\int_{\theta_S}^{\theta_P} \psi\, r\, d\theta\, dr}{\int_{r_H}^{r_T}\int_{\theta_S}^{\theta_P} r\, d\theta\, dr} = \frac{1}{S}\int_{r_H}^{r_T}\int_{\theta_S}^{\theta_P} \psi\, r\, d\theta\, dr \qquad (5)$$

and

$$<\psi> \equiv \frac{\int_{r_H}^{r_T}\int_{\theta_S}^{\theta_P} \rho\psi\, r\, d\theta\, dr}{\int_{r_H}^{r_T}\int_{\theta_S}^{\theta_P} \rho\, r\, d\theta\, dr} = \frac{\overline{\rho\psi}}{\bar{\rho}} \qquad (6)$$

and where flow tangency has been imposed at the hub, tip-shroud, and blade surfaces. S here denotes the passage cross-sectional area.

By applying the averaging procedure to the momentum equations (Eq. 2) in the relative cylindrical coordinates, the following equations are obtained:

(Axial-momentum)

$$\frac{\partial}{\partial t}(\bar{\rho} S <w_z>) + \frac{\partial}{\partial z}(\bar{\rho} S <w_z w_z> + \bar{p} S) = \int_{\theta_S}^{\theta_P} \Delta_r (pr\tan\phi)\, d\theta + \int_{r_H}^{r_T} \Delta_\theta (p\tan\beta)\, dr \qquad (7)$$

(Tangential-momentum)

$$\frac{\partial}{\partial t}(\bar{\rho} S \langle u_\theta r \rangle) + \frac{\partial}{\partial z}(\bar{\rho} S \langle w_z u_\theta r \rangle) = - \int_{r_H}^{r_T} \Delta_\theta(p) r \, dr \tag{8}$$

(Radial-momentum)

$$\frac{\partial}{\partial t}(\bar{\rho} S \langle w_r \rangle) + \frac{\partial}{\partial z}(\bar{\rho} S \langle w_z w_r \rangle) = - \int_{\theta_S}^{\theta_P} \Delta_r(pr) d\theta + \bar{\rho} S \left\langle \frac{(u_\theta r)^2}{r^3} + \frac{p/\rho}{r} \right\rangle \tag{9}$$

where $\tan\phi = \partial r/\partial z$ on the hub and shroud surface and $\tan\beta = r\partial\theta/\partial z$ on the blade surfaces. It was deemed appropriate—compare the time derivative and the convective flux terms—to express the flow field variables in terms of density-weighted averages and area-averages. Note that the averaged equations have been expressed in terms of the absolute velocity $\underline{u} = \underline{w} + r\Omega\hat{e}_\theta$ and the momentum equations are influenced weakly by the rotor speed through the equation of state

$$\left\langle \frac{p}{\rho} \right\rangle = (\gamma - 1)\left(\langle \tilde{e}_I \rangle - \frac{1}{2}\left[\langle \underline{w} \cdot \underline{w} \rangle - \langle (r\Omega)^2 \rangle\right]\right) \tag{10}$$

where $\langle p/\rho \rangle = \bar{p}/\bar{\rho}$.

Application of the passage-averaging procedure to the relative energy equation (Eq. 3) provides

$$\frac{\partial \bar{\rho} S \langle \tilde{e}_I \rangle}{\partial t} + \frac{\partial \bar{\rho} S \langle w_z \tilde{h}_I \rangle}{\partial z} = 0 \quad . \tag{11}$$

Relating Averaged-Products to Products of Averages

In application it is necessary to expand the averages of variable-products (*e.g.*, $\langle w_z w_r \rangle$) into products of averaged-variables (*e.g.*, $\langle w_z \rangle \langle w_r \rangle$). A deviation from the mean of an arbitrary variable f is defined as

$$f' \equiv f - \langle f \rangle = f - \frac{\overline{\rho f}}{\bar{\rho}} \quad . \tag{12}$$

By applying the passage averaging procedure, the following product relationships are obtained:

$$\langle fg \rangle = \langle f \rangle \langle g \rangle + \langle f' g' \rangle \tag{13}$$

and

$$\langle fgh \rangle = \langle f \rangle \langle g \rangle \langle h \rangle + \langle f' g' \rangle \langle h \rangle + \langle f' h' \rangle \langle g \rangle + \langle g' h' \rangle \langle f \rangle + \langle f' g' h' \rangle \quad . \tag{14}$$

By using these relationships to expand the density-averaged products in the conservation equations above, the passage-averaged equations are obtained:

$$\frac{\partial \underline{Q}}{\partial t} + \frac{\partial \underline{F}}{\partial z} = \frac{\partial \underline{F}'}{\partial z} + \underline{G} + \underline{G}' + \underline{L} \tag{15}$$

where

$$\underline{Q} = \bar{\rho} S \left[1, \langle w_z \rangle, \langle u_\theta r \rangle, \langle w_r \rangle, \langle \tilde{e}_I \rangle\right]^T \tag{16}$$

and

$$\underline{F} = \bar{\rho} S \begin{bmatrix} \langle w_z \rangle \\ \langle w_z \rangle \langle w_z \rangle + \langle p/\rho \rangle \\ \langle w_z \rangle \langle u_\theta r \rangle \\ \langle w_z \rangle \langle w_r \rangle \\ \langle w_z \rangle \langle \tilde{h}_I \rangle \end{bmatrix} \tag{17}$$

$$\underline{F}' = -\bar{\rho} S \begin{bmatrix} 0 \\ \langle w_z' w_z' \rangle \\ \langle w_z' (u_\theta r)' \rangle \\ \langle w_z' w_r' \rangle \\ \langle w_z' \tilde{h}_I' \rangle \end{bmatrix} \tag{18}$$

$$\underline{G} = \bar{\rho} S \begin{bmatrix} 0 \\ 0 \\ 0 \\ \langle u_\theta r \rangle^2 \langle 1/r^3 \rangle + \langle p/\rho \rangle \langle 1/r \rangle + G_4' \\ 0 \end{bmatrix} \tag{19}$$

with

$$G_4' = \langle (u_\theta r)' (u_\theta r)' (1/r)' \rangle + \langle (u_\theta r)' (u_\theta r)' \rangle \langle 1/r \rangle + 2\langle (u_\theta r)' (1/r)' \rangle \langle u_\theta r \rangle + \langle (p/\rho)' (1/r)' \rangle \tag{20}$$

and

$$\underline{L} = \begin{bmatrix} 0 \\ \int_{\theta_S}^{\theta_P} \Delta_r (pr\tan\phi)\,d\theta + \int_{r_H}^{r_T} \Delta_\theta (p\tan\beta)\,dr \\ -\int_{r_H}^{r_T} \Delta_\theta (p)\,r\,dr \\ -\int_{\theta_S}^{\theta_P} \Delta_r (pr)\,d\theta \\ 0 \end{bmatrix} \quad . \quad (21)$$

The blade and hub and tip-shroud force integrals must be modeled in order to apply the passage-averaged equations. The correlation terms too should be modeled or else shown to be negligible.

Force Integrals

The momentum equations are weakly coupled through the blade and hub and tip-shroud force integrals of Eq. 21. The force integrals are related to the pressure gradients sustained by acceleration induced by unsteadiness, flow turning, and rotational forces. Two approaches to close the system of equations are suggested here: a.) a local flow field can be postulated for the sake of deriving expressions for the force integrals of the three momentum equations; and b.) the three momentum equations can be collapsed through the force integrals into one effectively axial momentum equation.

Local Flow Sub-Model Approach

Consider the case of a gas dynamic wave propagating normal to the blades of a staggered, uncambered passage (see Figs. 1 and 2). For the sake of brevity in this discussion, radial variations are neglected and only the blade-to-blade (tangential) sub-model is considered here. Because $r\partial\theta/\partial z = 0$, $\partial p/\partial\eta = 0$. The local loading is therefore related to the axial gradient of the area-averaged pressure without approximation through

$$\Delta_\theta(p) = p_P - p_S = \sin\beta\cos\beta\,\frac{\partial \bar{p} S}{\partial z} \quad (22)$$

where β is used here to indicate the constant stagger angle. The axial and tangential momentum equations can then (in this very restrictive case) be rewritten as

$$\frac{\partial}{\partial t}(\bar{\rho} S \langle w_z \rangle) + \frac{\partial}{\partial z}(\bar{\rho} S \langle w_z w_z \rangle) + \frac{\partial}{\partial z}(\bar{p} S \cos^2\beta) = 0 \quad (23)$$

and

$$\frac{\partial}{\partial t}(\bar{\rho} S \langle u_\theta r \rangle) + \frac{\partial}{\partial z}(\bar{\rho} S \langle w_z u_\theta r \rangle) + \frac{\partial}{\partial z}(\bar{p} S r \cos\beta \sin\beta) = 0 \quad . \quad (24)$$

Although the sub-model approach is intended to retain the various momentum equations, note that if it is further assumed that locally $w_\theta = w_z \tan\beta$, then Eq. 24 is redundant and simply re-expresses continuity and axial momentum conservation.

It is beyond the scope of the present paper to develop a detailed sub-model for the force integrals; however, two ideas are formed from the above results. First, it is possible (in at least one case) to develop a sub-model for the local pressure distribution—in this example, $\partial p/\partial\eta = 0$—which can be used to relate the local loading to the axial gradient of area-averaged pressure. (Future work would be required to develop a generalized local flow sub-model, although it is unclear whether or not this a practical goal.) Second, the system of equations is reduced by relating the tangential and radial velocity components to the axial velocity component. This approach is used below.

"One-Dimensional" Model Approach

By relating the density-averaged tangential and radial velocity components to the density-averaged axial velocity component via specified area-averaged flow-tangent axial distributions, the axial loading term L_2 can be related to the tangential and radial loading terms L_3 and L_4, and the three momentum equations can be folded into a single axial momentum equation. If the correlation terms are neglected (for the moment), then the blade force integral of the axial momentum equations can be expanded into

$$\int_r \Delta_\theta (p\tan\beta)\,dr \approx \overline{\tan\beta}\int_{r_H}^{r_T} \Delta_\theta (p)\,dr + \bar{p}\int_{r_H}^{r_T} \Delta_\theta (\tan\beta)\,dr \quad (25)$$

and the hub and tip-shroud force integral can be expanded into

$$\int_\theta \Delta_r (pr\tan\phi)\,d\theta \approx \overline{\tan\phi}\int_{\theta_S}^{\theta_P} \Delta_r (pr)\,d\theta + \overline{pr}\int_{\theta_S}^{\theta_P} \Delta_r (\tan\beta)\,d\theta \quad (26)$$

where it is also assumed that $\overline{pr} = \bar{p}\,\bar{r}$. The momentum

equations are related through the force integrals and can be folded together by assuming that

$$\frac{\langle w_\theta \rangle}{\langle w_z \rangle} = \overline{\tan\beta} \approx \frac{1}{2}(\tan\beta|_P + \tan\beta|_S) \qquad (27)$$

and

$$\frac{\langle w_r \rangle}{\langle w_z \rangle} = \overline{\tan\phi} \approx \frac{1}{2}(\tan\phi|_T + \tan\phi|_H) \quad . \qquad (28)$$

It is noted that the error introduced in these assumptions is likely on the order of the error incurred by neglecting the correlation terms. Under these assumptions, the passage-averaged equations can be written as

$$\frac{\partial}{\partial t}\begin{bmatrix} \bar{\rho} S \\ \bar{\rho} S \langle w_z \rangle \delta^2 \\ \bar{\rho} S \langle \tilde{e}_i \rangle \end{bmatrix} + \frac{\partial}{\partial z}\begin{bmatrix} \bar{\rho} S \langle w_z \rangle \\ \bar{\rho} S \langle w_z \rangle^2 \delta^2 + \bar{p} S \\ \bar{\rho} S \langle w_z \rangle \langle \tilde{h}_i \rangle \end{bmatrix} = \begin{bmatrix} 0 \\ G_2 \\ 0 \end{bmatrix} \qquad (29)$$

where

$$\delta^2 \equiv 1 + \overline{\tan\beta}^2 + \overline{\tan\phi}^2 \quad . \qquad (30)$$

and where

$$G_2 \approx \bar{\rho} S [\, \overline{\tan\phi}\, \Omega^2 \langle r \rangle + \frac{\langle w_z \rangle^2}{2} \frac{\partial \delta^2}{\partial z}] + \bar{p} S \frac{\overline{\tan\phi}}{\langle r \rangle} + \bar{p} S [\, \frac{\Delta_r(\tan\phi)}{r_T - r_H} + \frac{\Delta_\theta(\tan\beta)}{\bar{r}(\theta_P - \theta_S)}] \quad . \qquad (31)$$

Equations 29-31 represent a closed set of effectively one-dimensional equations that account for the influence of blade, hub, and tip-shroud profiling. The source term, Eq. 31, evidently contains the influence of rotation and blade, hub, and tip-shroud surface profiling on the rotor flow. Note that by applying Eq. 29 in the restricted case of a passage with constant-radius hub and tip-shroud surfaces and uncambered blades at stagger (*i.e.*, $\delta^2 = 1/\cos^2\beta$ and $G_2 = 0$), Eq. 23 is recovered. Further, the classical quasi-one-dimensional equations are recovered in the limiting case of $\delta^2 = 1$ and $\overline{\tan\phi} = \overline{\tan\beta} = 0$.

Correlation Terms

The correlation terms (*e.g.*, $\langle w_z' w_r' \rangle$) were introduced by the expansion of the density-average of variable-products ($\langle w_z w_r \rangle$) into products of the density-averaged variables ($\langle w_z \rangle \langle w_r \rangle$). These passage-averaged "stress" terms are non-zero if there are instantaneous pitchwise or spanwise variations in the product constituents (w_z and w_r). The variations are induced in general by a.) acceleration caused by relative unsteadiness, relative flow turning, rotational forces, and shear forces and b.) entropy nonuniformities due to the presence of shock waves or contact discontinuities oriented other than normal to the *z*-axis, heat transfer, and wakes. Although the local values of the correlation terms may be large, it is predominantly the axial gradients of these terms that impact the momentum and energy balances. The radial momentum equation is further influenced by the correlation terms arising from the radial source terms (*i.e.*, G_4' of Eqs. 19 and 20).

The magnitudes of the correlation terms and their axial gradients depend on the direction over which the governing equations are averaged. That is, the correlation terms are not invariant through a coordinate transformation. Consider the flow fields schematically depicted in Figs. 1-3. For brevity, the discussion is again restricted to constant radius; it is conceptually simple to extend the analysis to account for spanwise variations in the flow field. The three scenarios each depict a gas dynamic wave that separates a reference state 0 which is at rest relative to the rotor from a state 1 in which flow is either entering or exiting the rotor passage. If gas dynamic waves in wave rotor passages were to always propagate with orientations that were normal to the blade surfaces (as depicted in Figs. 1 and 2), then the passage-averaging might optimally be applied along surfaces oriented normal to the rotor surfaces (*i.e.*, constant-ξ lines in Figs. 1 and 2 and constant-μ lines in Fig. 3). By averaging in the intrinsic (ξ, η) coordinates, the magnitude of the correlation terms and their streamwise gradients would be minimized; indeed, an averaging carried out along constant-ξ lines in an uncambered passage geometry (Figs. 1 and 2) would lead to no correlation terms at all. This would hold both for both steady and unsteady flows because the transverse (η) gradients would be zero in the uncambered passages. The relative flow turning of cambered passages (*e.g.*, see Fig. 3) establishes transverse gradients that give rise to finite correlation terms, even if the passage-averaging is carried out in the intrinsic coordinates. The streamwise gradients of these correlation terms would still be zero in regions where the flow is locally steady (*i.e.*, $\partial/\partial t = 0$), for example, fore and aft of the expansion fan in Fig. 3. But, unlike the uncambered passage, the streamwise gradients of the correlation terms are non-zero in the unsteady flow regions of passages with surface-profiling-induced, relative, flow turning.

The above discussion might seemingly motivate an averaging procedure in intrinsic coordinates; however, in general the gas dynamic waves do not propagate oriented normal to the rotor surfaces; rather, the wave

orientation is influenced by the gradual opening and closing of the rotor passages, the passage geometry, and wave refraction caused by temperature and velocity nonuniformities (*e.g.*, at contact discontinuities). Therefore, there seemed little impetus to formulate the passage-averaged equations in intrinsic coordinates. It is noted however, that having carried out the averaging procedure at constant z-lines, the gradients of the correlation terms are also non-zero wherever there are local spanwise or pitchwise nonuniformities, including regions of steady flow turning.

In the following sections, the influence of the correlation terms is discussed by using analytical solutions for idealized gas dynamic wave propagation in representative wave rotor passage geometries.

Shock Wave in a Staggered, Uncambered Passage

Consider a shock wave propagating into a gas at rest relative to a wave rotor passage defined by the staggered, uncambered blades shown in Fig. 1. The net force established by the shock wave is a constant in time, $F_\theta = -p_0 L_R r_T (1 - r_H/r_T)(p_1/p_0 - 1)\sin\beta/\sigma)$. The net force is due to the difference between the pressure forces on the pressure and suction sides of the blades in the instantaneous "shadow" of the shock ($0 \le z^* \le 1$). By inspection it is evident that the correlation terms are non-zero in this same region because the shock wave is oriented at an angle relative to the averaging surface. The flow is locally steady ($\partial/\partial t = 0$) outside of this region and the correlation terms are zero. The extent of the shadow of the shock relative to the chord length is $\sin\beta/\sigma$. By considering that typical wave rotor solidities (σ) are between 10 and 20 and that inflow and outflow blade angles are as high as $|\beta| \le 45°$, it is evident that the shock wave could induce correlation terms over a significant (*e.g.*, 10%) portion of the rotor passage.

The magnitude of the correlation term for two arbitrary variables f and g in the vicinity of the shock is given by

$$\frac{\partial(\bar{\rho} S \langle f' g' \rangle)}{\partial z} = \frac{\begin{pmatrix} \Delta_\theta(\rho f g) + \langle g \rangle \langle f \rangle \Delta_\theta(\rho) \\ -\langle f \rangle \Delta_\theta(\rho g) - \langle g \rangle \Delta_\theta(\rho f) \end{pmatrix}}{\sin\beta \cos\beta} \quad (32)$$

The correlation terms are locally related to the tangential (pitchwise) differences (Δ_θ) in the flow field variables at the averaging surface which are established by the shock wave. The tangential difference terms in Eq. 32 can be obtained by using the following shock relationships: $\delta(\rho w_\xi) = w_{SH}\delta(\rho)$ and $\delta(\rho w_\xi^2 + p) = w_{SH}\delta(\rho w_\xi)$. The relative magnitudes of the correlation terms can then be attained by using

$$\frac{\partial_z(\bar{\rho} S \langle w_\xi' w_\xi' \rangle)}{\partial_z(\bar{\rho} S \langle w_\xi^2 \rangle)} = \frac{1 - \gamma \dfrac{\rho_0/\rho_1 - 1}{p_1/p_0 - 1}\left(\dfrac{\langle w_\xi \rangle - w_{SH}}{a_0}\right)^2}{1 - \gamma \dfrac{\rho_0/\rho_1 - 1}{p_1/p_0 - 1}\left(\dfrac{w_{SH}}{a_0}\right)^2}. \quad (33)$$

The relative shock speed, w_{SH}, and the density ratio, ρ_1/ρ_0, are functions of the shock strength, p_1/p_0. The relative magnitudes of the correlation terms vary with shock strength and axial position (because $\langle w_\xi \rangle$ varies axially). Evidently, the gradients of the correlation terms are on the same order of magnitude as the local gradient of the inviscid flux in the vicinity of the shock wave.

Expansion from a Staggered, Uncambered Passage

Consider an expansion wave propagating into a gas at rest relative to a wave rotor passage defined by staggered, uncambered blades shown in Fig. 2. By neglecting end effects, the expansion wave propagates oriented normal to the blades as shown and the flow field is uniform along the isobars shown. The simple wave spreads linearly with time; however, the loading established by the expansion fan is a constant in time ($F_\theta = p_0 L_R r_T (1 - r_H/r_T)(1 - \epsilon)\sin\beta/\sigma$), like the shock wave considered earlier.

The correlation terms for the uncambered passage are zero fore and aft of the expansion fan where the flow is locally steady (*i.e.*, $\partial/\partial t = 0$). The correlation terms are non-zero in the regions of unsteadiness established by the expansion fan (*i.e.*, $0 \le z^* \le 1$ of Fig. 2). Their magnitudes again depend on the tangential differences at the averaging plane instantaneously established by the expansion wave (cf. Eq. 32). Unlike the shock wave, the tangential differences decrease with time in the case of the expansion fan and must be obtained from the time-dependent flow field solution.

The streamwise velocity within the expansion fan (see Fig. 2) is

$$\frac{w_\xi(\xi, t)}{a_0} = \frac{2}{\gamma + 1}\left[\frac{(\xi - \xi_0)}{L_T}\frac{t_0}{t} - 1)\right] \quad (34)$$

where $t_0 = L_T/a_0$ and where ξ_0 is the position of the expansion fan at $t = 0$. The intrinsic and cylindrical coordinates are related by

$$\frac{\xi - \xi_0}{L_T} = \frac{\lambda_1}{\lambda_0}\frac{t}{t_0}(1 - z^*) + \frac{z^* t}{t_0} - \frac{\sin\beta}{\sigma}\left(z^* - \frac{\theta_P - \theta}{\theta_P - \theta_S}\right) \quad (35)$$

where $\lambda_1/\lambda_0 = 1 + \frac{\gamma+1}{\gamma-1}[\epsilon^{(\gamma-1)/2\gamma} - 1]$ is the ratio of the wave speeds fore and aft of the expansion fan and where the normalized axial position ($z^* = (z-z_{min})/(z_{max}-z_{min})$) is defined in Fig. 2. Aft of the expansion fan, the local velocity is $w_{\xi,0}/a_0 = \frac{2}{\gamma+1}(\lambda_1/\lambda_0 - 1)$ which depends on the expansion fan pressure strength ($\epsilon = p_1/p_0$). The relative velocity in front of the expansion fan is zero. The local speed of sound is related to the local streamwise velocity component through

$$\frac{a(\xi,t)}{a_0} = 1 + \frac{\gamma-1}{2}\frac{w_\xi(\xi,t)}{a_0} \qquad (36)$$

and the local static pressure, p/p_0, is isentropically related to the local speed of sound.

The relative magnitude of the correlation term gradients (*e.g.*, $\partial_z(\bar{\rho}S\langle w'w'\rangle)/\partial_z(\bar{\rho}S\langle w^2\rangle)$) were calculated numerically by using the flow field described above. The expansion fan spreads with time; therefore, the magnitude of the local pressure gradient, and hence the flow field nonuniformity, decreases with time. The relative magnitude of the gradient of a correlation term at a fixed normalized position ($0 \le z^* \le 1$) within the expansion fan is a function of the ratio of specific heats (γ), the expansion fan strength (ϵ), the stagger angle ($\sin\beta$), the passage solidity (σ), and time ($a_0 t/L_T$). At early times, the relative magnitudes of the correlation terms are of order unity at the ends of the expansion fan and approach the significant levels of the shock wave considered in the previous section. In general, the relative magnitudes of the axial gradients of the correlation terms ($\partial_z(\bar{\rho}S\langle w_z'w_z'\rangle)/\partial_z(\bar{\rho}S\langle w_z^2\rangle)$) inside the expansion fan decrease with time ($\sim (a_0 t/L_T)^{-3/4}$, see Fig. 4), decrease with solidity ($\sim \sigma^{-0.8}$, see Fig. 5), and increase with stagger angle ($\sim \sin^2\beta$, see Fig. 6). At times greater than the (normalized) blade passing period ($a_0/(r\Omega\sigma)$), the relative magnitudes of the axial gradients of the correlation terms are small ($\mathcal{O}$ 0.1%) except at the head of the expansion fan where the local relative velocity is nearly zero. It is therefore expected to be a good approximation to neglect the correlation terms introduced by averaging procedure in a flow field established by a simple expansion fan, except at early times when the simple model problem posed here is invalidated by the passage gradual opening and closing (*i.e.*, end) effects.

Expansion from Circular Arc, Unstaggered Passage

Consider an expansion wave propagating into a gas at rest relative to a rotor passage defined by two concentric circular arcs as shown in Fig. 3. The propagation of the expansion wave is a complicated, multi-dimensional process which is beyond the scope of the present work to describe; however, it is interesting to consider the scenario depicted schematically in Fig. 3 in the light of the earlier discussion of the expansion fan in the uncambered passage.

The correlation terms are zero in the quiescent flow (state 0) fore of the expansion fan. The propagating expansion fan establishes pitchwise and spanwise gradients, and hence non-zero correlation terms. The magnitudes of the correlation terms will depend upon the local acceleration which has two components in the case of the cambered passage: a.) the streamwise, μ-gradient of pressure which depends on the expansion fan strength (ϵ) and which is expected to decay strongly with time ($a_0 t/L_T$); and b.) the transverse, R-gradient which is influenced by the local flow turning. In the circular arc geometry, it is expected that following the flow transient induced by the expansion fan, the radial component of velocity, w_R, will soon relax to zero. When $w_R = 0$, the flow behaves locally like a free vortex flow in which $\partial P/\partial R = \rho w_\mu^2/R$ and $w_\mu \sim 1/R$. In such regions (*e.g.*, state 1, aft of the expansion fan), it is expected that the relative magnitudes of the gradients of the correlation terms will increase with both the passage radius-ratio (R_P/R_S) and radius-to-arc-length ratio (or normalized radius of curvature, R_S/L_R). If the circular arc blades were staggered, the stagger angle would likely influence the correlation terms as well through its influence on the instantaneous "shadow" of the wave. Note that although the flow is locally steady aft of the expansion fan, because of the averaging surfaces chosen in this work, and in contrast to the staggered, uncambered passage case, the axial gradients of the correlation terms are non-zero in state 1: the correlation terms impact the passage-averaged momentum and energy balances in the portions of the passage in which steady flow turning takes place.

Question of Need to Model Correlation Terms

The question of whether or not it is imperative to include the correlation terms to attain the accuracy required for engineering problems was not answered by the present study. Although beyond the scope of the present paper, future work should assess the importance of the correlation terms in the following stepwise fashion: first, while neglecting the correlation terms, the inviscid flow in a passage defined by two concentric circular arcs should be computed by using the "one-dimensional" model provided in the present work; the obtained flow solution should be compared with results from a multi-dimensional flow solver (*e.g.*, Ref. 6) and the accuracy of the one-dimensional solution assessed. If the instantaneous solutions of the two solution methods agree, then for the purpose of wave rotor

design and analysis studies, the correlation terms can be neglected. If however the results are significantly different, then the correlation terms might in fact be relatively important. In this case, a generalized model for the correlation terms should be developed and validated by using results from multi-dimensional simulations.

Summary

The governing equations for an inviscid flow in cylindrical coordinates fixed to the spinning rotor were passage-averaged by integrating from hub to tip and from blade to blade. The averaging was motivated by the need for a reduced set of governing equations appropriate for the parametric analyses of wave rotor design studies. Application of the passage-averaged equations requires closure models for blade, hub, and tip-shroud force integrals and for correlation terms. In one of the force-integral models considered, the three momentum equations were collapsed into a single, effectively axial, momentum equation by relating the density-averaged tangential and radial velocity components to the density-averaged axial velocity component, under the constraint that the flow travels along a path inferred from the rotor geometry. This approach yielded an essentially one-dimensional formulation suitable for a CFD-based analysis tool for wave rotors with generalized rotor passage geometries. It remains for future work to implement and to validate this formulation. The validation can be carried out by comparing the predictions of the implemented model with results from a multi-dimensional solver.

Correlation terms arise in the application of the passage-averaged equations when the density-average of products of the flow field variables are expanded into products of the density-averaged variables. The magnitudes of the correlation terms and their gradients are influenced by the orientation of the averaging surface. In the present work, the correlation terms are non-zero if there are spanwise or pitchwise flow field variations caused by either local entropy gradients or flow acceleration. Acceleration can be established by a.) relative unsteadiness, b.) relative flow turning induced by blade, hub, and tip-shroud profiling, and c.) rotation. The influences of relative unsteadiness on the correlation terms were analyzed by considering the idealized problems of shock and expansion waves propagating in staggered, uncambered passages. The relative magnitudes of the axial gradients of the correlation terms can be on the order of the axial gradients of the inviscid fluxes in the portions of the rotor passage influenced by the gas dynamic waves. Relative flow turning induced by the profiling of the rotor passage surfaces also establishes pitchwise and spanwise gradients, and hence correlation terms.

References

[1]Azoury, P. H., *Engineering Applications of Unsteady Flow*, Wiley, New York, 1992.

[2]Welch, G. E., Jones, S. M., and Paxson, D. E., "Wave-Rotor-Enhanced Gas Turbine Engines," *J. Engineering for Gas Turbines and Power*, **119**, No. 2, April, 1997, pp. 469-477.

[3]Lear, W. E., Jr. and Kielb, R. P., "The Effect of Blade Angle Design Selection on Wave-Turbine Engine Performance," ASME-96-GT-259, June, 1996.

[4]Welch, G. E., "Wave Engine Topping Cycle Assessment," AIAA-97-0707, Jan., 1997; also NASA TM-107371 and ARL-TR-1284, Jan., 1997.

[5]Paxson, D. E., "Comparison Between Numerically Modeled and Experimentally Measured Wave-Rotor Loss Mechanisms," *J. Propulsion and Power*, **11**, No. 5, Sept.-Oct., 1995, pp. 908-914.

[6]Welch, G. E., "Two-Dimensional Computational Model for Wave Rotor Flow Dynamics," ASME-96-GT-550, June, 1996; also NASA TM-107192 and ARL-TR-924, Mar., 1996.

[7]Larosiliere, L. M., "Wave Rotor Charging Process: Effects of Gradual Opening and Rotation," *J. Propulsion and Power*," **11**, No. 1, Jan.-Feb., 1995, pp. 178-184.

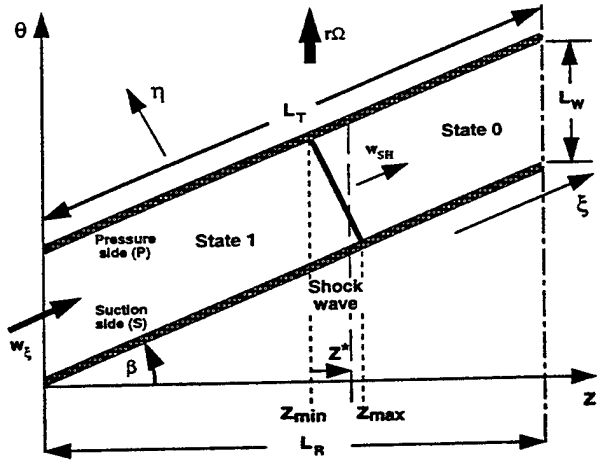

Figure 1. Schematic diagram of a shock wave propagating into gas at rest relative to a wave rotor passage defined by staggered, uncambered blades (blade-to-blade view).

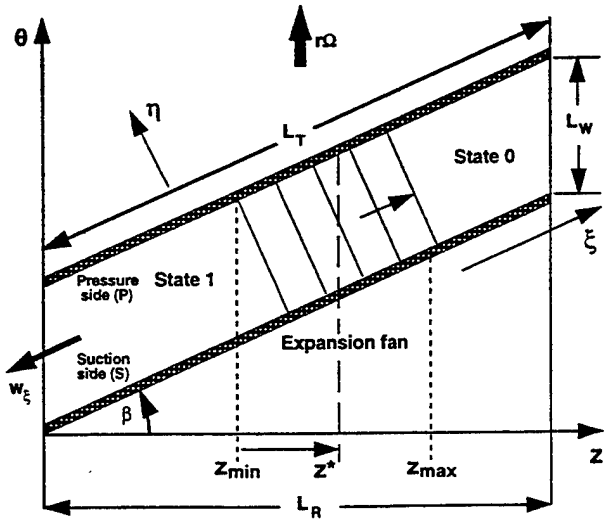

Figure 2. Schematic diagram of an expansion fan propagating into gas at rest relative to a wave rotor passage defined by staggered, uncambered blades (blade-to-blade view).

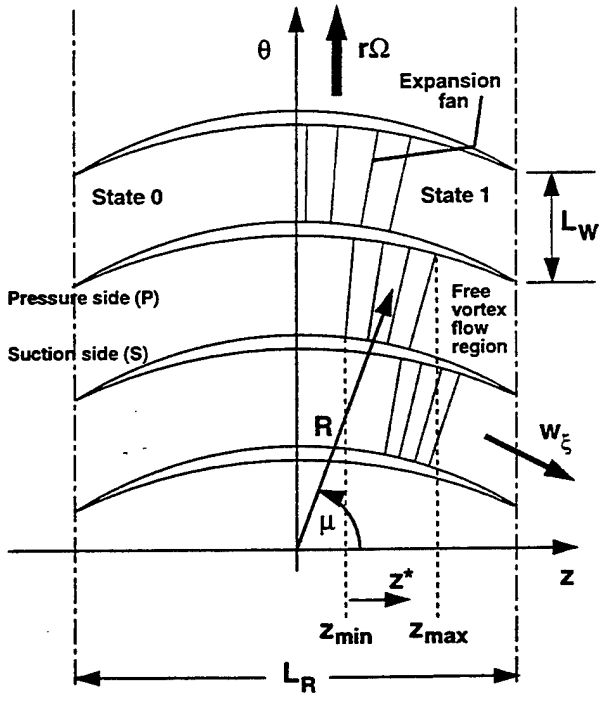

Figure 3. Schematic diagram of expansion fans propagating into gas at rest relative to wave rotor passages defined by unstaggered, circular arc (cambered) blades (blade-to-blade view).

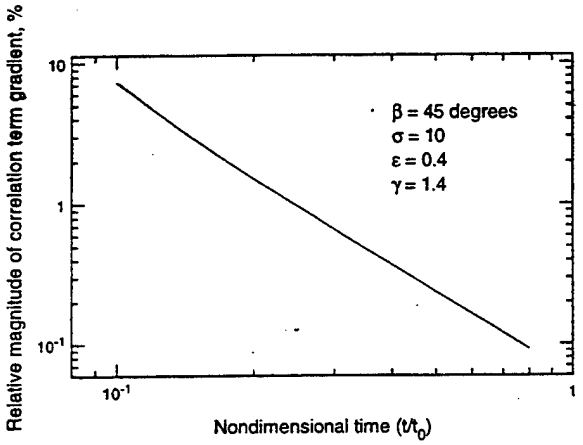

Figure 4. Relative magnitude of the gradient of the correlation terms of the axial momentum equation, at nondimensional axial position (z^*) in expansion fan, as a function of nondimensional time (t/t_0).

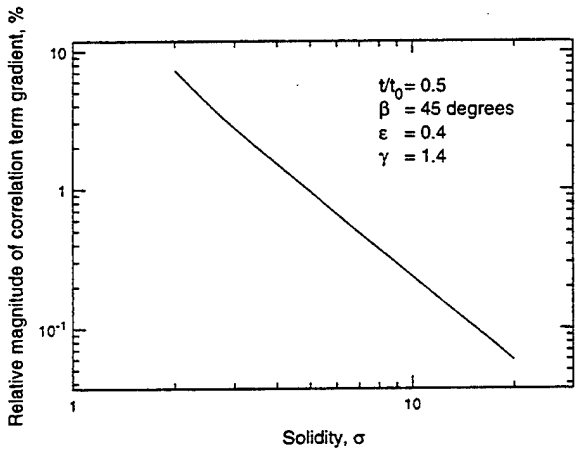

Figure 5. Relative magnitude of the gradient of the correlation terms of the axial momentum equation, at nondimensional axial position (z^*) in expansion fan, as a function of solidity (σ).

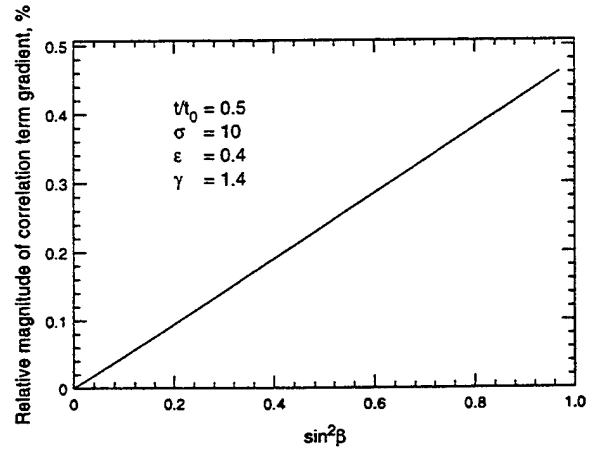

Figure 6. Relative magnitude of the gradient of the correlation terms of the axial momentum equation, at non-dimensional axial position (z^*) in expansion fan, as a function of blade angle (β).

REPORT DOCUMENTATION PAGE

Form Approved
OMB No. 0704-0188

1. AGENCY USE ONLY (*Leave blank*)	2. REPORT DATE	3. REPORT TYPE AND DATES COVERED
	July 1997	Technical Memorandum

4. TITLE AND SUBTITLE

Passage-Averaged Description of Wave Rotor Flow

5. FUNDING NUMBERS

WU–505–26–33

6. AUTHOR(S)

Gerard E. Welch and Louis M. Larosiliere

7. PERFORMING ORGANIZATION NAME(S) AND ADDRESS(ES)

NASA Lewis Research Center
Cleveland, Ohio 44135–3191
and
U.S. Army Research Laboratory
Cleveland, Ohio 44135–3191

8. PERFORMING ORGANIZATION REPORT NUMBER

E–10822

9. SPONSORING/MONITORING AGENCY NAME(S) AND ADDRESS(ES)

National Aeronautics and Space Administration
Washington, DC 20546–0001
and
U.S. Army Research Laboratory
Adelphi, Maryland 20783–1145

10. SPONSORING/MONITORING AGENCY REPORT NUMBER

NASA TM–107518
ARL–TR–1462
AIAA–97–3144

11. SUPPLEMENTARY NOTES

Prepared for the 33rd Joint Propulsion Conference and Exhibit cosponsored by AIAA, ASME, SAE, and ASEE, Seattle, Washington, July 6–9, 1997. Responsible person, Gerard E. Welch, organization code 5810, (216) 433–8003.

12a. DISTRIBUTION/AVAILABILITY STATEMENT

Unclassified - Unlimited
Subject Category 07

This publication is available from the NASA Center for AeroSpace Information, (301) 621–0390.

12b. DISTRIBUTION CODE

13. ABSTRACT (*Maximum 200 words*)

The unsteady flow within wave rotor passages is influenced by the rotor blade, hub, and tip-shroud surface profiles. By averaging from hub to shroud and from blade to blade, a reduced set of the governing equations is obtained that is appropriate for design studies and parametric analyses. The application of these equations requires closure models for force integrals and for correlation terms that arise when the density-averages of products of the flow field variables are expanded in terms of products of the density-averaged variables. The force integrals and the correlation terms depend on the instantaneous pitchwise and spanwise flow field distributions established by unsteadiness relative to the rotor, flow turning induced by blade, hub, and tip-shroud profiling, and rotation. Two approaches to model the force integrals are described. The influence of relative unsteadiness and flow turning on the correlation terms is discussed by considering the propagation of gas dynamic waves in rotor passages defined by uncambered, staggered blades and by unstaggered, cambered blades.

14. SUBJECT TERMS

Wave rotor; Wave engine; Modeling; Turbomachinery; Gas turbine engine

15. NUMBER OF PAGES

11

16. PRICE CODE

A03

17. SECURITY CLASSIFICATION OF REPORT	18. SECURITY CLASSIFICATION OF THIS PAGE	19. SECURITY CLASSIFICATION OF ABSTRACT	20. LIMITATION OF ABSTRACT
Unclassified	Unclassified	Unclassified	